International Journal of Nanomedicine

Dovepress
open access to scientific and medical research

Open Access Full Text Article

ORIGINAL RESEARCH

Overcoming multidrug resistance through inhalable siRNA nanoparticles-decorated porous microparticles based on supercritical fluid technology

This article was published in the following Dove Press journal:
International Journal of Nanomedicine

Pei-Yao Xu[1,2]
Ranjith Kumar Kankala[1–3]
Yu-Jing Pan[1,2]
Hui Yuan[1,2]
Shi-Bin Wang[1–3]
Ai-Zheng Chen[1–3]

[1]College of Chemical Engineering, Huaqiao University, Xiamen 361021, P. R. China; [2]Institute of Biomaterials and Tissue Engineering, Huaqiao University, Xiamen 361021, P. R. China; [3]Fujian Provincial Key Laboratory of Biochemical Technology (Huaqiao University), Xiamen 361021, P. R. China

Background: In recent times, the co-delivery therapeutics have garnered enormous interest from researchers in the treatment of cancers with multidrug resistance (MDR) due to their efficient delivery of multiple agents, which result in synergistic effects and capable of overcoming all the obstacles of MDR in cancer. However, an efficient delivery platform is required for the conveyance of diverse agents that can successfully devastate MDR in cancer.

Methods: Initially, short-interfering RNA-loaded chitosan (siRNA-CS) nanoparticles were synthesized using the ionic gelation method. Further, the siRNA-CS nanoparticles and doxorubicin hydrochloride (DOX) were co-loaded in poly-L-lactide porous microparticles (PLLA PMs) (nano-embedded porous microparticles, [NEPMs]) by the supercritical anti-solvent (SAS) process.

Results and discussion: The NEPM formulation exhibited an excellent aerodynamic performance and sustained release of DOX, which displayed higher anticancer efficacy in drug-resistant cells (human small cell lung cancer, H69AR cell line) than those treated with either free DOX and DOX-PLLA PMs due to the siRNA from CS nanoparticles silenced the MDR gene to DOX therapy.

Conclusion: This eco-friendly process provides a convenient way to fabricate such innovative NEPMs co-loaded with a chemotherapeutic agent and a gene, which can devastate MDR in cancer through the co-delivery system.

Keywords: pulmonary delivery, short-interfering RNA, multidrug resistance, doxorubicin, supercritical carbon dioxide

Introduction

With the cumulative incidences over the past few decades, lung cancer has become a leading cause of cancerous deaths worldwide, due to uncontrolled proliferation rate of cells and poor prognosis instigated by drug resistance.[1–3] Currently, various therapeutic strategies, chemotherapy alone or in combination with other strategies such as radiation and surgical practices, are available for the treatment of lung cancer.[4–6] However, the clinical application of these conventional chemotherapeutic strategies has been limited due to the complicated and diversiform mechanisms of multidrug resistance (MDR) attained by cells, including the overexpression of MDR-associated proteins (MRPs/ABCCs) in ATP-binding cassette (ABC) transporter family and permeability glycoprotein on the cell surface.[4,5,7–9] In addition, several cases of cancer cells exhibit MDR phenotype, which restricts the entry of drugs through various

Correspondence: Ai-Zheng Chen
College of Chemical Engineering, Huaqiao University, Xiamen 361021, P. R. China
Tel +86 592 616 2326
Fax +86 592 616 2326
Email azchen@hqu.edu.cn

submit your manuscript | www.dovepress.com
Dovepress
http://dx.doi.org/10.2147/IJN.S169399

mechanisms, resulting in the distortion of therapeutic dosage regimen.[4,5] These consequences often drive clinicians toward the administration of multiple chemotherapeutic drugs at higher doses resulting in the severe adverse effects.[10] These issues have led the researchers toward the development of various innovative formulations, which can efficiently inhibit MDR through diverse agents and subsequently enhance the drug levels.[11]

In the past decade, the tremendous progress has evidenced the development of numerous agents that significantly inhibit MDR through various mechanisms. In this context, short-interfering RNA (siRNA) offers significant potential by downregulating the expression of cell surface efflux ABC family, through specifically silencing a broad range of their preceding genetic targets and subsequently enhancing the internalization efficiency of chemotherapeutic agents.[12] Furthermore, a combination of chemotherapy and gene therapy through codelivery of an anticancer drug and an MDR-restricting siRNA will be more effective in devastating MDR in cancer, by targeting different cellular signaling pathways and reducing the doses of chemotherapeutic drugs by overcoming MDR.[13–15] However, the formulation of siRNA and its delivery specifically for cancer therapy is highly challenging, due to quick degradation and rapid renal clearance of naked siRNA (without the use of delivery vectors), resulting in the significant loss of its bioactivity.[16] Currently, many types of siRNAs in combination with the anticancer drugs and their complexes have been delivered using various nanocarriers for efficient accumulation in cancer cells by both passive and active targeting, ensuring the high drug concentrations at the tumor site with improved efficiency.[17–19] However, only a fraction of anticancer drugs could reach the tumor sites in the lung after they were administered through the traditional administration procedures, such as oral and intravenous routes.[20,21] To address these limitations, the localized delivery of chemotherapeutic agent and siRNA directly via inhalation systems to the lung tumor is highly desirable for enhancing their therapeutic efficacy and for subsequently lowering the systemic undesired side effects.[22,23] By doing so, inhalation systems can deliver siRNA directly to the lungs, which can retain the stability of siRNA after release due to lower nuclease activity in the airways.[24]

Pulmonary delivery through inhalable particulate systems, such as metered dose inhalers and dry powder inhalers, holds considerable potential in drug delivery due to its significant advantages such as superior chemical stability, uniform dosage, and no specific requirement of coordination of inhalation with activation, among others.[25,26] Despite the advantages and success in the synthesis and codelivery of anticancer drugs and siRNA by nanomedicine platform, the nanocarriers still face a significant limitation for lung cancer treatment, ie, rapid exhalation before reaching the site of action due to their small size (<0.5 μm).[27–29] However, the inhalation microparticles with geometric size (1–3 μm) and mass density (~1 g/cm^3) by various conventional manufacturing methods tend to aggregate in the dry powder inhaler leading to nonuniformity in dispensed doses and substantially prone to rapid clearance by macrophages in the lumen, which significantly reduce the efficacy of several anticancer drugs.[30] To overcome these limitations, polymer-based porous microparticles (PMs) with an appropriate geometric size have been utilized for the delivery of various therapeutic agents in the lungs owing to their attractive properties such as low aerodynamic density (<0.4 g/cm^3) and adaptive aerodynamic diameter (1–5 μm), among others.[31,32] Polymers with excellent biocompatibility and biodegradation such as poly(lactic-*co*-glycolic) acid (PLGA)- and poly-L-lactide (PLLA)-based microparticles showed intended applications for pulmonary delivery due to their option of tailoring their rate of drug release without causing tissue damage in the lungs.[33,34] Herein, nano-embedded porous microparticles (NEPMs) as inhalation delivery systems offer unique advantages over other carriers including nonviral gene vectors in overcoming MDR such as synergistic delivery efficacy and physicochemical attributes of both nanoparticles and microparticles, and high deposition rate in the alveoli facilitating the transport of nanoparticles to the target site in the lungs and enhancing the availability, stability, and efficacy of nanoparticles.[28,35] Moreover, the matrix of NEPMs dissolves in the lung's epithelial lining fluid after inhalation, resulting in the sustained release of drug and nanoparticles from these porous architectures.[36] Different approaches have been explored for preparing inhalable dry powders, such as spray drying,[37] micronization,[38] and supercritical fluid (SCF) technology.[39] Among various methods available, the SCF technology holds a great promise in polymer processing by making use of benign solvents, in particular, supercritical carbon dioxide (SC-CO_2) that is operated at moderate critical conditions (temperature, 31.1°C and pressure, 73.8 bar).[40,41] In addition, this eco-friendly technology is beneficial in producing PMs with minimal organic solvent residues in the end product.[40] Herein, SC-CO_2 acts as an antisolvent in the supercritical antisolvent (SAS) process, which has shown great progress in producing micro- and nano-sized polymeric composites for pulmonary delivery.[40,42,43]

In this article, we present an innovative design of inhalable PMs possessing doxorubicin hydrochloride (DOX) and siRNA for reversing the MDR of lung cancer through the codelivery approach. Initially, the siRNA-loaded chitosan (siRNA-CS) nanoparticles were fabricated through the ionic gelation method, and further, these nanoparticles as well as a chemotherapeutic agent, DOX, were encapsulated into PLLA PMs by the SAS process. These siRNA-CS nanoparticles-embedded PLLA PMs (siRNA-CS-DOX-PLLA PMs, or shortly denoted as NEPMs) possessing unique properties of both nanoparticles and microparticles (1–5 μm) for codelivery of a gene and a chemotherapeutic agent are highly suitable for deep lung deposition, and releasing the nanoparticles for the intracellular delivery of siRNA and escaping the phagocytosis by macrophages after reaching the deeper lung tissues.[44–46] In addition, the delivered siRNA from the CS nanoparticles effectively obstructs MDR through the gene silencing effect and subsequently enhances the uptake of DOX released from the NEPMs (Figure 1).

Materials and methods

Chemicals and reagents

siRNA (sense, 5′-GCAGACCUCUUCUACUCUUTT-3′ and antisense, 5′-AAGAGUAGAAGAGGUCUGCTT-3′) specific to human MRP-1 and negative control (NC) siRNA (sense, 5′-UUCUCCGAACGUGUCACGUTT-3′ and antisense, 5′-ACGUGACACGUUCGGAGAATT-3′) and FAM-labeled siRNA (FAM-siRNA) were purchased from Gene Pharma Co. Ltd. (Shanghai, China). Fluorescein isothiocyanate (FITC) and DOX was obtained from Aladdin Co. Ltd. (Shanghai, China). PLLA was purchased from Jinan Daigang Biomaterial Co. Ltd. (Jinan, China). CS, sodium tripolyphosphate (TPP), Pluronic F-127 (PF-127), ammonium bicarbonate (AB), and dichloromethane (DCM) were purchased from Sigma-Aldrich Co. (St Louis, MO, USA). CO_2 (purity >99.9%, v/v) was supplied by Xiamen Rihong Co., Ltd. (Xiamen, China). Roswell Park Memorial Institute medium (RPMI-1640), fetal bovine serum (FBS), and dimethyl sulfoxide (DMSO) were obtained from GIBCO/BRL

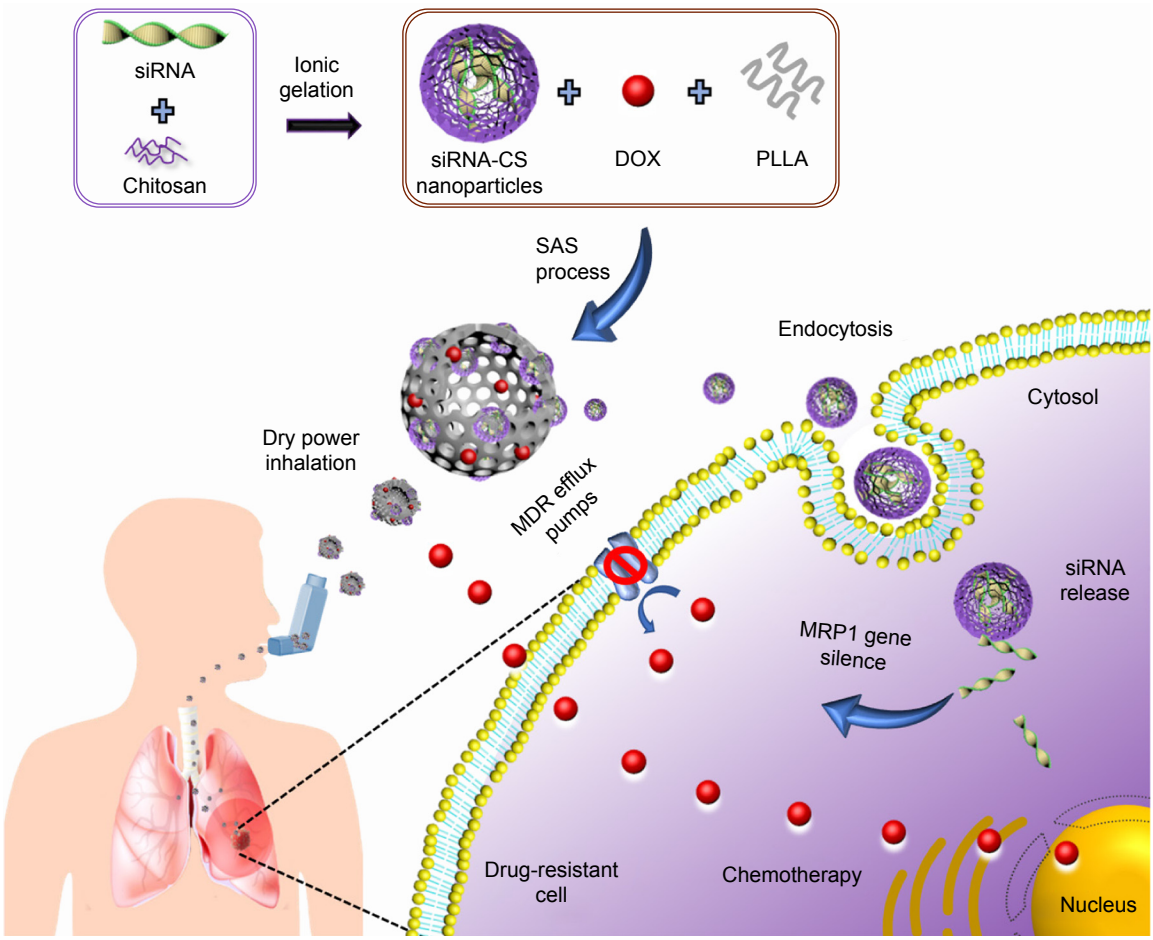

Figure 1 Schematic illustration representing the outline of synthesis and pulmonary codelivery of DOX and MRP1 siRNA.
Abbreviations: DOX, doxorubicin hydrochloride; MDR, multidrug resistance; MRP, MDR-associated proteins; PLLA, poly-L-lactide; siRNA, short-interfering RNA; siRNA-CS, siRNA-loaded chitosan; SAS, supercritical antisolvent.

Life Technologies (Grand Island, NY, USA). 4′6-Diamidino-2-phenylindole (DAPI) and LysoTracker Red were obtained from KeyGen BioTECH Co. Ltd (Jiangsu, China).

Physical characterization

The surface morphology of the nanoparticles, as well as PMs, was characterized by field emission scanning electron microscopy (FE-SEM, S-4800 UHR; Hitachi, Tokyo, Japan). The samples were prepared by depositing an aqueous solution of the sample (10 µL) onto the conducting resin mica grid before coating a thin layer of gold. The particle size distribution and zeta potential of CS nanoparticles and siRNA-CS nanoparticles were determined using the dynamic light scattering (DLS) method using Zetasizer Nano ZS (Zeta PALS; Malvern Instruments Ltd., Malvern, UK). The influence of the SAS process on the functional groups of the materials was estimated by Fourier transform infrared spectroscopy (FTIR) (Nicolet iS50; Thermo Fisher Scientific, Waltham, MA, USA). The geometric mean diameter (D_g) and particle size distribution of microparticles were measured using a laser diffraction particle size analyzer (LS320, Beckman Coulter Inc, CA, USA). To further determine the distribution of nanoparticles in PMs, FITC-conjugated CS (FITC-CS) nanoparticles were synthesized as reported previously and characterized using a confocal laser scanning microscope (CLSM, CarlZeiss LSM510; Carl Zeiss Meditec AG, Jena, Germany).[32] The aerosolization behavior of NEPMs was captured by a digital video camera (Canon; Tokyo, Japan) at 0.04 second intervals after actuation.

Preparation of NEPMs

Initially, siRNA-CS nanoparticles were prepared by the ionic gelation method, in which the positively charged amino groups of CS interact with the negatively charged TPP, and then these nanoparticles along with DOX were dispersed over PLLA PMs using the SAS process. siRNA-CS nanoparticles were prepared by following the procedure given below.[47] siRNA (optical density – 2.0, 66 µg) was dissolved in 250 µL of TPP solution (1 mg/mL) and then added to 500 µL of CS solution (2 mg/mL). The siRNA-CS nanoparticles were harvested by gentle vortexing for a minute.

To obtain uniform-sized NEPMs through the SAS process, it is required to prepare an emulsion containing oil and water phases. Initially, the water phase was prepared by dissolving DOX and suspending siRNA-CS nanoparticles in 2 mL of saturated solution of AB. On the other hand, as presented in the process conducted before, the required oil phase was prepared by dissolving 306.6 mg of PLLA and 153.3 mg of PF-127 in 20 mL of DCM.[39,48] Next, 2 mL of water phase was added to 20 mL of oil phase under ultrasonication to obtain homogeneous water in oil emulsion, and then the mixture was subjected to SAS processing at adjusted critical conditions.

The precipitation experiments of NEPMs and CS nanoparticles-embedded PLLA microparticles (CS-PLLA PMs) were carried out in a SAS apparatus (SN3937782; Waters, MA, USA), which has been described elsewhere (Figure 2).[48,49] In brief, CO_2 was cooled to 4°C before being compressed to a liquid and preheated in a heat exchanger prior to spraying it into the precipitation chamber or high-pressure vessel. Simultaneously, the homogeneous emulsion mixture was injected at a flow rate of 4.0 mL/min into the precipitation chamber (500 mL) at stabilized operating conditions (pressure, 8 MPa; temperature, 30°C; the flow rate of CO_2, 40 mL/min) through a steel nozzle (inner diameter of 0.006 inches). In the end, the SC–CO_2 was sprayed at the adjusted operating conditions for excess 30 minutes for washing the residual content of organic solvent in the microparticles. The microparticles were eventually collected from the high-pressure vessel and dried using the vacuum at 50°C for 2 hours to decompose AB.

Aerodynamic properties

The practical deposition of NEPMs into the lung can be correlated by measuring the aerodynamic properties of the samples.[50] The aerodynamic performance of NEPMs was measured by using an eight-stage Andersen Mark II cascade impactor (ACI 20–810; Thermo Fisher Scientific). The composites of NEPMs (10 mg) were loaded into the capsules through the induction port into the ACI at a flow rate of 28.3 L/min for 60 seconds. The effective cutoff aerodynamic diameter (D_a) at each stage of the ACI was as follows: Stage 0, 9 µm; Stage 1, 5.8 µm; Stage 2, 4.7 µm; Stage 3, 3.3 µm; Stage 4, 2.1 µm; Stage 5, 1.1 µm; Stage 6, 0.65 µm; Stage 7, 0.43 µm; and Stage 8, $<$0.43 µm. Finally, D_a was calculated by measuring the weight of the powder at each stage before and after the release of capsules. In addition, the fine particle fraction (FPF) was determined by the interpolation of the percentage of the particles containing less than 5 µm.

Drug loading and encapsulation efficiency

To determine the DOX loading and encapsulation efficiency in NEPMs, 10 mg of NEPMs was dissolved in 500 µL of DCM and then diluted to 20 mL with phosphate sodium acetate buffer (pH 7.4). The mixture was then shaken thoroughly to completely remove the remnants of DCM. The sample was filtered, and the supernatant was then collected and analyzed by ultraviolet-visible (UV-Vis)

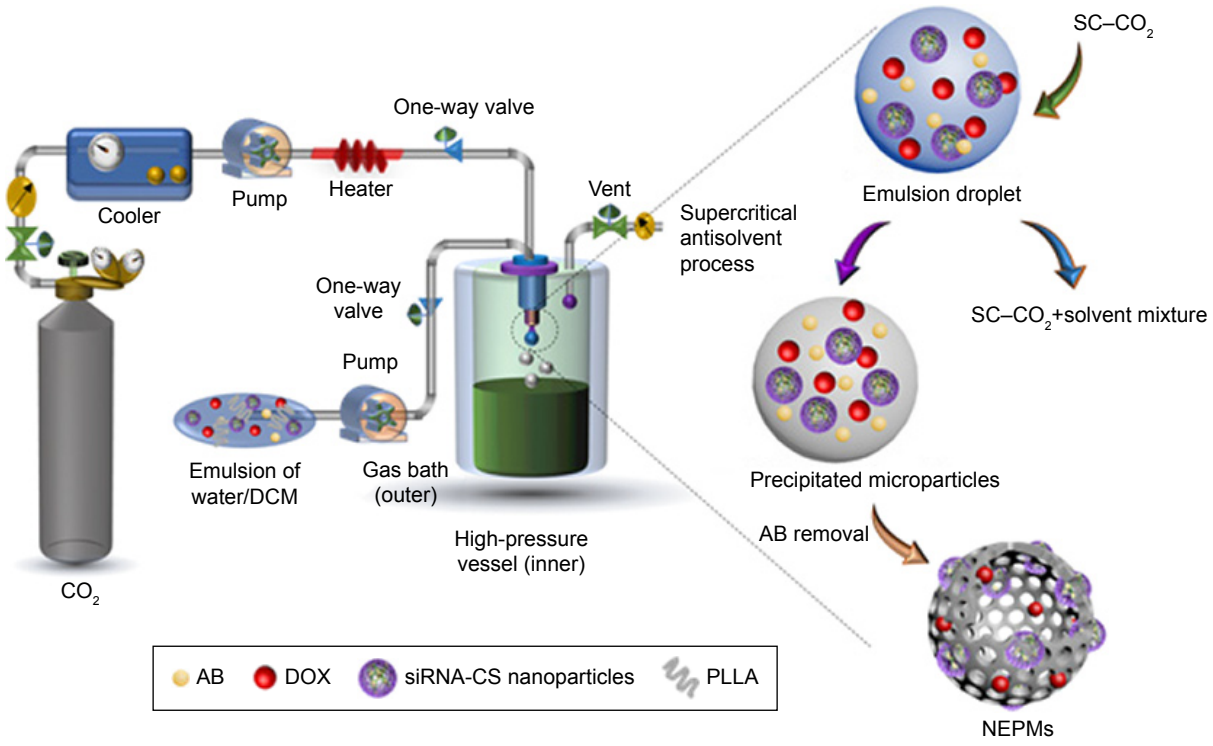

Figure 2 Schematic illustration demonstrating the instrument setup of SAS process and the mechanistic elucidation of particle formation.
Notes: Within the high-pressure vessel, rapid mixing and diffusion at the outlet interface of SC–CO_2 and the emulsion mixture occur instantaneously. At the same time, the polymer and drug in the emulsion mixture become supersaturated, and the solute undergoes nucleation and subsequent precipitation, resulting in the formation of PMs containing AB as a gas-foaming porogen. Finally, the drying process completely removes the AB, yielding the highly porous architectures.
Abbreviations: AB, ammonium bicarbonate; PM, porous microparticle; SAS, supercritical antisolvent.

spectrophotometer (UV-1800; Shimadzu, Kyoto, Japan) at 480 nm. The drug load amount is generally determined from the mass ratio of the active pharmaceutical ingredient to the carrier, while the encapsulation efficiency is defined as the mass ratio of the encapsulated drug to the initial amount of drug taken. The drug load and the encapsulation efficiency were calculated using the following equations.

$$\text{Drug load (\%)} = \frac{W_1}{W_2} \times 100 \quad (1)$$

$$\text{Encapsulation efficiency (\%)} = \frac{W_1}{W_3} \times 100 \quad (2)$$

where W_1, W_2, and W_3 represent the total weight of DOX in NEPMs, the gross weight of NEPMs, and the weight of initial DOX considered for the fabrication process, respectively.

In vitro drug release

The drug release experiments were conducted using the dialysis method. Typically, the samples of NEPMs with different loading amounts (5%, 7.5%, and 10% w/w of NEPMs) of DOX (10 mg, 2 mg/mL) were suspended in the dialysis bags separately (molecular weight cutoff 7,000), and they were then placed in a bottle with 20 mL of phosphate-buffered saline (PBS, pH 7.4) and kept in a shaker maintained at 37°C. At predetermined intervals, 5 mL of sample aliquots were collected, and the concentration of DOX was analyzed using a UV-Vis spectrophotometer at 480 nm. The release experiments were continued by replenishing an equal volume of the fresh buffer after each sampling. In addition, the dissolution of free DOX was conducted as control by using the same method. On the other hand, siRNA release from CS nanoparticles was also investigated separately using the following procedure for avoiding the influence of DOX, as it results in the absorption peak at around 260 nm. siRNA-CS nanoparticles were suspended in 1 mL of PBS buffer and were then placed in an arbitrary shaker (70 rpm, 37°C). At scheduled time intervals, the suspensions were centrifuged at 15,000 rpm for 10 minutes. Furthermore, the amount of released siRNA in the supernatant was determined by ultramicro spectrophotometer at 260 nm. Each experiment was carried out in triplicate.

Cellular internalization efficiency

The human small cell lung cancer cells (H69AR, MDR cell line) were obtained from American Type Culture Collection

(ATCC, Manassas, VA, USA). Cells were cultured in RPMI-1640 supplemented with 20% of FBS, 1% penicillin, and 1% streptomycin. The cells were incubated in a humidified atmosphere (5% CO_2, 37°C).

The delivery efficacy of NEPMs was evaluated using the cellular uptake study through the visualization of auto-fluorescent DOX in CLSM (TCS SP8; Leica Microsystems, Wetzlar, Germany). The H69AR cells were harvested after 80% of confluence and seeded onto a 24-well plate at a density of 1×10^5 cells per well and incubated for 24 hours for proper cell attachment. The media from the wells were then replaced with free DOX, NC NEPMs, and NEPMs dispersed in the FBS-free media at a concentration of 8 µg of DOX/mL. After 24 hours of incubation, the medium was pirated, and the cells were washed twice with PBS. Furthermore, the cells were attached to the bottom of the plate by incubating with the paraformaldehyde (4%) for 15 minutes, stained with DAPI for 10 minutes, with intermittent PBS washes, and then observed under CLSM. To assess the endosomal/lysosomal escape of siRNA-CS nanoparticles, the FAM-siRNA (100 nM) was incubated with H69AR cells for 6 hours. Subsequently, the cells were washed thrice with PBS followed by staining with LysoTracker Red for 30 minutes for visualizing the endosomes/lysosomes, and then the stained cells were observed using CLSM imaging.

Anticancer study

The effect of various designed constructs of NEPMs on the cell viability of H69AR cells was assessed by MTT assay.[51] Cells were seeded at a density of 1×10^4 cells per well of a 96-well plate and incubated overnight for proper cell attachment. The medium was then replaced with fresh medium containing the indicated formulations (free DOX, NC NEPMs, DOX-PLLA PMs, NEPMs), and the cells were incubated for another 24 hours. Furthermore, the medium was pirated and replaced with MTT (5 mg/mL, 20 µL) reagent diluted with 80 µL of RPMI-1640 and incubated for 4 hours at 37°C. The MTT solution was then pirated, and the obtained formazan precipitate was dissolved in DMSO (150 µL/well). The dissolved formazan absorbance was eventually measured using a microplate reader at 570 nm (Multiskan EX; Thermo Fisher Scientific). The mouse fibroblast cells (L929) were obtained from ATCC. The cell viability test of CS-PLLA PMs was evaluated using L929 to explore the biocompatibility in vitro.

Results and discussion

The chief aim of the material design (Figure 2) is to develop NEPMs by an eco-friendly process based on the SCF technology for lung cancer therapeutics. DOX and MRP1 siRNA were chosen as a model chemotherapeutic agent and a gene, respectively, to synergistically conquer MDR through this inhalation codelivery system. We have synthesized NEPMs by initially preparing siRNA-CS nanoparticles using the ionic gelation method, and they were then dispersed along with DOX on PMs using the SAS process. Furthermore, these NEPMs were systematically characterized using various techniques such as SEM for demonstrating the surface morphology of PMs, fluorescence imaging for elucidating the distribution of nanoparticles over PMs, and aerodynamic properties of PMs for validating their delivery through the pulmonary route. Then, the DOX and siRNA release studies, cellular uptake efficiency in vitro, and lysosomal escape study of siRNA were performed to corroborate the delivery efficacy of PMs and nanoparticles. Eventually, we report the cell viability study in MDR cell line for evaluating the therapeutic anticancer effects of the NEPM design in comparison with free DOX.

Physical characterization

The surface morphology of the siRNA-CS nanoparticles, as well as their subsequent NEPM design, was observed using SEM (Figure 3A). Uniform-sized spherical structures of siRNA-CS nanoparticles with an average diameter of around 100 nm were produced by the ionic gelation method. These tiny nanocomposites are appropriate in size for loading into the PMs and are also highly suitable for the cellular internalization through endocytosis for gene silencing effect. Furthermore, the loading efficiency of siRNA in CS nanoparticles was estimated as 77.4%, which is indeed very high. The high loading efficiency of the gene is attributed to not only the electrostatic interactions between negatively charged siRNA and positively charged CS but also physical entrapment upon the ionic crosslinking induced by TPP.[52] As compared to the zeta potential value of CS nanoparticles (34.6 mV) obtained by DLS measurements, the decrease in zeta potential after siRNA loading demonstrates the successful formation of siRNA-CS nanoparticles (21.3 mV) (Figure 3B).[53] Thus, these CS nanoparticulate forms act as an efficient carrier of genes. Furthermore, the delivery efficiency of these CS nanoparticles was evaluated by investigating the release of siRNA in vitro in the simulated physiological buffer using a UV-Vis spectrophotometer. Interestingly, these spherical CS nanoarchitectures have exhibited the sustained release behavior of siRNA (~60% in 24 hours) (Figure 3C). Moreover, the FTIR recordings further confirmed the DOX existence in PMs. The DOX sample has shown peaks at 1,728 and 1,233 cm^{-1} attributed to N–H stretching and

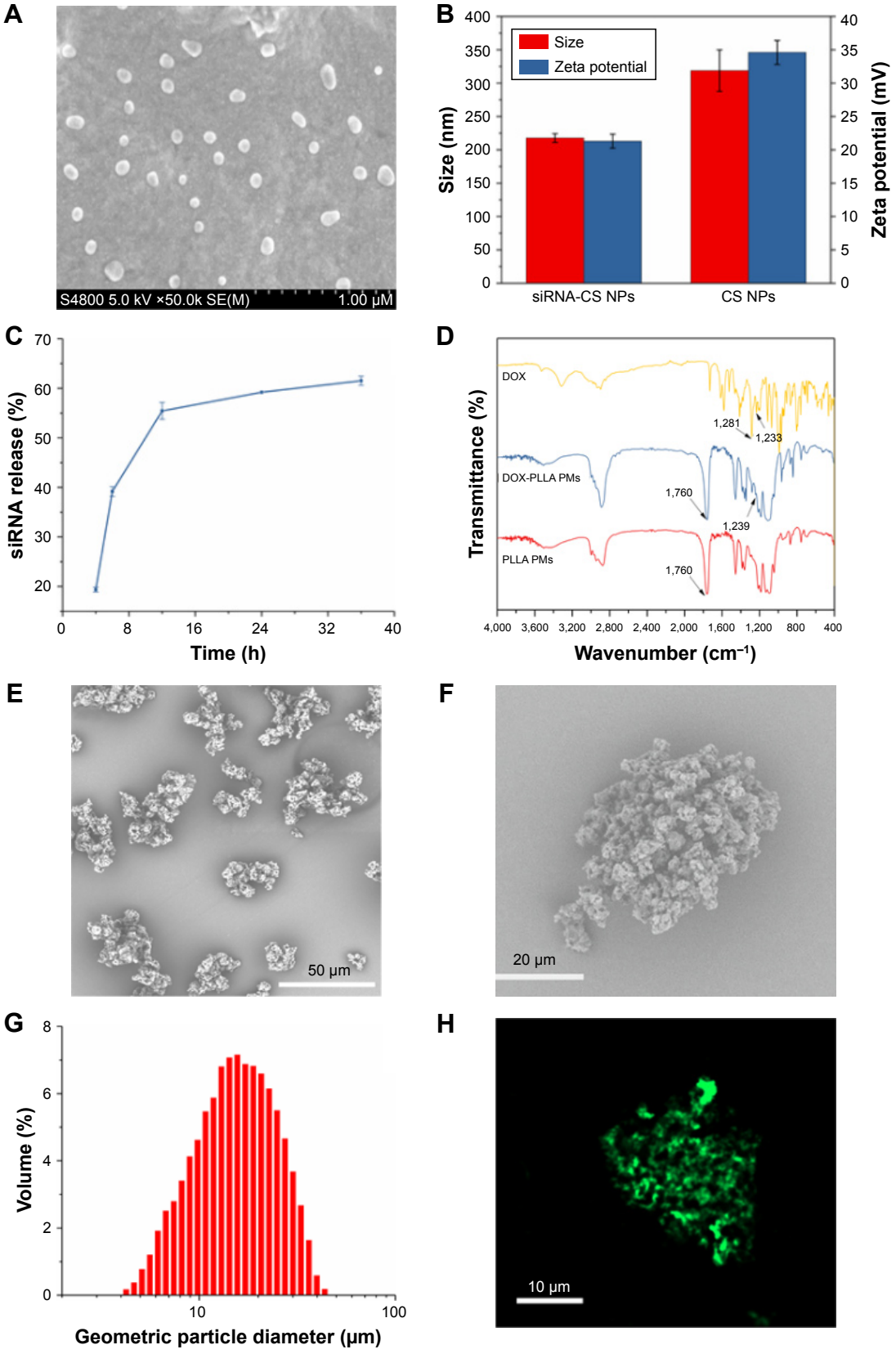

Figure 3 Physical characterization of NEPMs.

Notes: (**A**) SEM image of siRNA-CS nanoparticles, (**B**) Zeta potential and size of siRNA-CS nanoparticles and CS nanoparticles, (**C**) graphical representation illustrating the sustained release behavior of siRNA from the CS nanoparticles, (**D**) FTIR spectra of the raw DOX, PLLA PMs, and DOX-PLLA PMs, (**E**–**F**) SEM image of NEPMs, (**G**) particle size distribution of NEPMs measured by laser diffraction particle size analyzer, and (**H**) CLSM image illustrating the distribution of FITC-CS nanoparticles on PLLA PMs.

Abbreviations: CLSM, confocal laser scanning microscope; DOX, doxorubicin hydrochloride; FTIR, Fourier transform infrared spectroscopy; NEPM, nano-embedded porous microparticle; PLLA, poly-L-lactide; PM, porous microparticle; SEM, scanning electron microscopy; siRNA-CS, short-interfering RNA-loaded CS.

C–H stretching vibrations, respectively. In addition, the peak at 1,281 cm^{-1} was due to O–H–O, C–H, and C–OH stretching of DOX.[54] Indeed, the sharp and intense peaks at 1,760 cm^{-1} in PLLA PMs and DOX-PLLA PMs were identified as the characteristic stretching absorption of C=O bond of PLLA.[55] Compared to the FTIR curves of raw DOX and PLLA PMs, the absorption peaks (1,281 cm^{-1}) of the DOX-PLLA PMs were stronger. Furthermore, compared with PLLA PMs, a new peak at 1,239 cm^{-1} of DOX-loaded PLLA PMs (Figure 3D).

The morphological features of the eventual design of NEPMs produced by the SAS process were visualized through SEM observations. This eco-friendly SAS process resulted in the polymeric porous structures (Figure 3E–F) with an average geometric particle size of 16.86 µm (Figure 3G) and considerable rough surface, indicating the deposition of nanoparticles throughout the polymeric constructs. These porous architectures with optimum size and uniform distribution of nanoparticles over the surface could be easily transported by air and more efficiently penetrated through the lung capillaries. Furthermore, the distribution of nanoparticles over the PMs was confirmed by utilizing the FITC-CS nanoparticles for tracking them by CLSM. As depicted in Figure 3H, the green fluorescence emitted by FITC-CS nanoparticles indicates that the CS nanoparticles were well distributed throughout the PMs. The reasons behind the successful encapsulation of CS nanoparticles would be the optimized critical parameters of SC-CO_2 that favored their entrapement in PMs at the high-pressure conditions.

Aerodynamic properties

It is evident that the aerodynamic properties of drug delivery vehicles play a crucial role in the formulation as well as the delivery of drugs from the inhalation delivery system. More often, the microparticles with an average D_a >5 µm have a maximum possibility of their deposition in the oral cavity and pharynx, while the particles with the smaller D_a (<0.5 µm) are exhaled before their deposition in the airways. Therefore, the particles with D_g >10 µm and D_a ranged 1–5 µm are optimum, and thus, these parameters are highly suitable for the efficient deposition of particles in the airways.[56] In addition to the aerodynamic properties of particles, some other parameters also play a significant role in formulating the inhalation delivery systems such as drug dosage and proportion of the dose that are likely to enter the lungs. FPF is significantly considered in addressing these issues and substantially correlated with the therapeutic efficacy of the delivery system. The resultant aerodynamic properties, ie, D_g, D_a, and FPF, of NEPMs that were prepared at the different mass ratios of DOX are shown in Table 1. The results have shown that there is no significant change in both D_a and D_g with the increasing amount of DOX, and these parameters are slightly higher compared with the naked PMs (ie, PMs devoid of DOX). As mentioned earlier, the D_g of CS-PLLA PMs and NEPMs higher than 10 µm, D_a between 1 and 5 µm, and FPF >50% are optimum for the inhalation delivery.

Table 1 Aerodynamic properties of NEPMs at various theoretical amounts of DOX (n=3)

DOX amount (%)	D_g (µm)	D_a (µm)	FPF (%)
–	16.32±0.45	4.07±0.37	58.28±2.10
5.0	17.57±0.88	4.58±0.39	59.16±3.21
7.5	16.90±0.64	4.39±0.18	57.29±2.57
10.0	17.43±1.51	4.63±0.26	55.15±4.49

Abbreviations: DOX, doxorubicin hydrochloride; FPF, fine particle fraction; NEPM, nano-embedded porous microparticle.

Furthermore, the aerosolization behavior of the NEPMs was visually observed by capturing the pictures of actuation with an optical camera for every 0.04 seconds intervals. As shown in Figure 4, the aerosolization performance of NEPMs at the theoretical DOX loading amount of 7.5% was accomplished in 0.12 seconds after actuation, displaying good mobility in the air. Our results of actuation were in agreement with the reported literature. In one case, Kim et al designed PLGA PMs for exploring the initial aerosolization of particles and delivery efficacy in vivo. They reported that these PMs with optimum size had exhibited an excellent aerodynamic mobility for ~0.12 seconds after actuation. In addition, these PLGA PMs had successfully delivered human serum albumin (HSA) in vivo.[57]

In vitro DOX release

Prior to the release experiments, we have calculated the loading and encapsulation efficiencies of the drug in the matrix of PLLA PMs at different theoretical loading amounts of DOX. As depicted in Figure 5A, the loading efficiency of DOX was increased proportionally with its theoretical loading amount. By contrast, the encapsulation efficiency of DOX has initially increased proportionally to the loading amount but later reduced at the highest loading amount, (10%), but it still stands at around 50%–70% in all the circumstances. These consequences demonstrate that the entrapment of the drug molecules within the polymer matrix is limited during the SAS processing even at the higher theoretical amounts of drug encapsulation. However, the loading

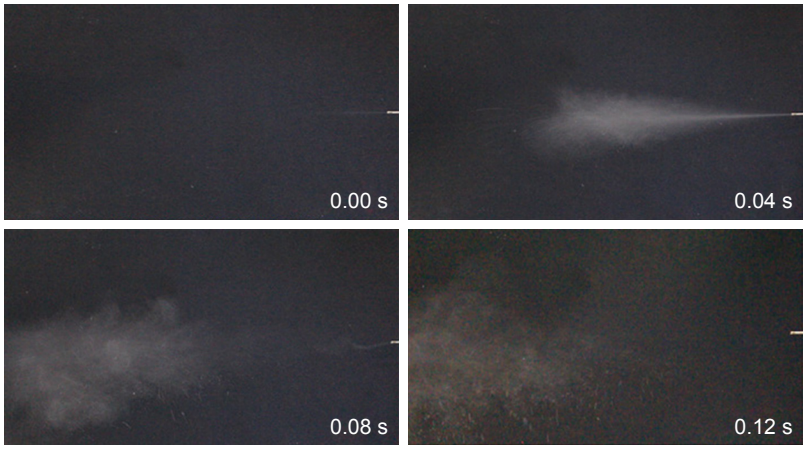

Figure 4 Images representing the aerosolization behavior of NEPMs using a dry powder insufflator.

and encapsulation efficiencies of DOX in PMs remained sufficient for its delivery and subsequent therapeutic efficacy. Another interesting feature of this NEPM formulation is the sustained delivery of DOX from the PLLA PMs. To explore this characteristic feature, the release behavior of DOX from PLLA PMs loaded at various theoretical loading amounts was investigated by measuring the drug concentration at predetermined intervals using a UV-Vis spectrophotometer (Figure 5B). The samples of NEPMs have shown the sustained release behavior of DOX compared with that of free DOX dissolution study under the same conditions provided. These PMs exhibited the initial rapid burst release of DOX during the first 2 hours, due to the swift diffusion of the DOX molecules adsorbed on their surface and/or the release of the encapsulated DOX close to the surface of PMs.[58] Entrapped DOX molecules that stayed firmly inside the NEPMs exhibited a relatively slow release (60%–80% for 60 hours), and the dominating factor in the release process of entrapped DOX could be drug diffusion and initial polymer degradation on the surface in the simulated physiological buffers.[59] It is evident from the results that the DOX release from the highly porous NEPMs can be sustained for days, which would be beneficial for long-term delivery of chemotherapeutic agents to the lungs.

Cellular internalization study

To explore the delivery efficacy of NEPMs, we investigated the subcellular localization of various constructs, ie, DOX-PLLA PMs, NC NEPMs, and NEPMs, along with free DOX in H69AR cancer cells using the CLSM study.[6] As depicted in Figure 6, the amounts of DOX fluorescence were aggregated significantly higher at the nuclei proximity of the

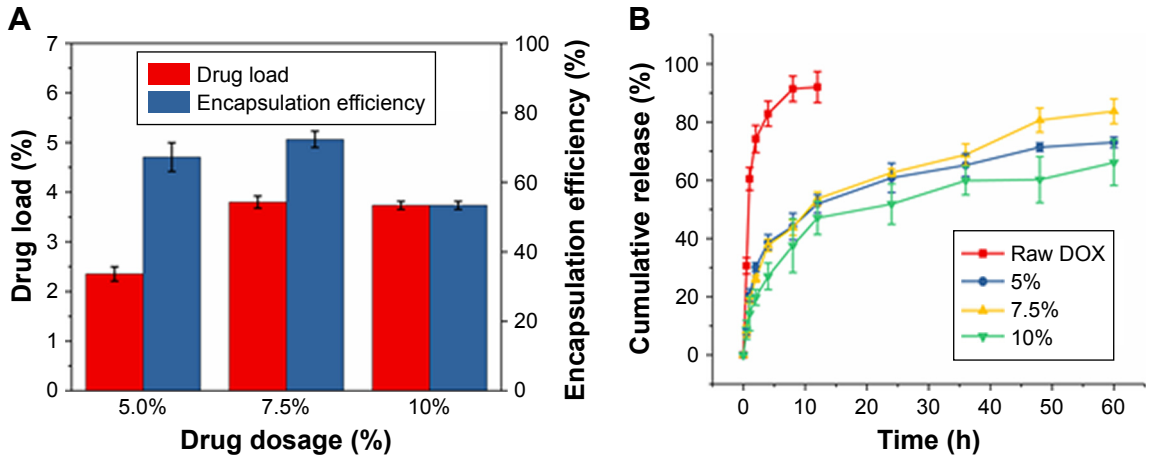

Figure 5 DOX loading and its release characteristics from PMs.
Notes: (**A**) DOX drug load and encapsulation efficiencies of NEPMs at various theoretical loading amounts; (**B**) cumulative DOX release characteristics of NEPMs in PBS (pH 7.4).
Abbreviations: DOX, doxorubicin hydrochloride; NEPMs, nano-embedded porous microparticles; PM, porous microparticle; PBS, phosphate-buffered saline.

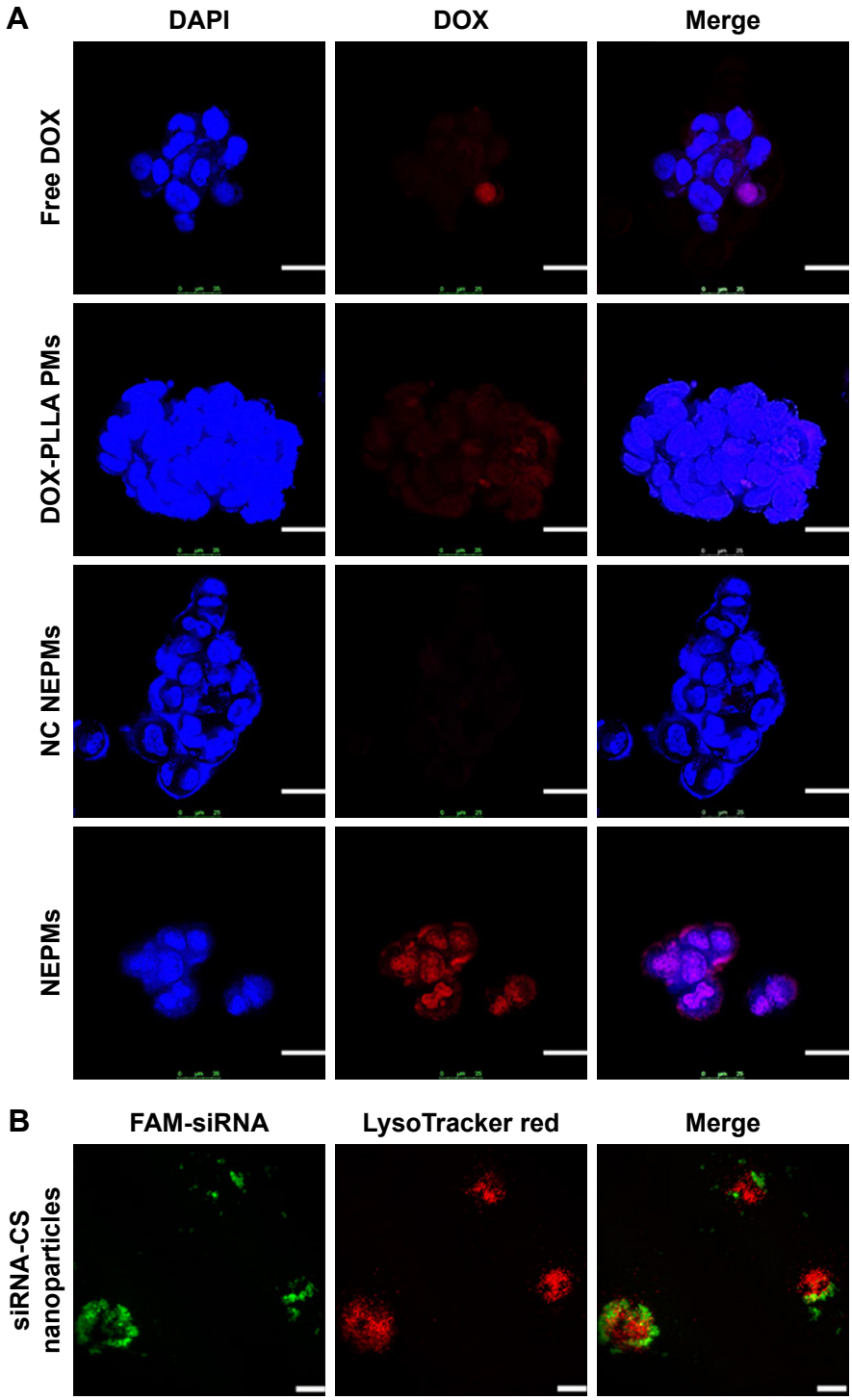

Figure 6 Cellular internalization of NEPMs.
Notes: (**A**) Fluorescence visualization of DOX representing its intracellular accumulation after the treatment of H69AR cancer cells with various constructs. Blue: DAPI stained nucleus; red: DOX. (**B**) CLSM images of H69AR cancer cells treated with siRNA-CS nanoparticles. Green: FAM-siRNA; red: LysoTracker Red stained lysosome (scale bar, 25 μm).
Abbreviations: CLSM, confocal laser scanning microscope; DAPI, 4′6-diamidino-2-phenylindole; DOX, doxorubicin hydrochloride; NC, negative control; FAM-siRNA, FAM-labeled siRNA; NEPMs, nano-embedded porous microparticles; PM, porous microparticle; siRNA-CS, short-interfering RNA-loaded CS.

NEPMs-treated cells compared with that of other samples (DOX-PLLA PMs and NC NEPMs) and free DOX. It is evident that the fluorescence of DOX is even higher in the NEPMs treatment compared with the NC NEPMs due to the specific gene silencing effect by MRP1 siRNA and eventual release of DOX that internalized the cells in a sustained fashion. On the contrary, the fluorescence intensity of DOX was very low in free DOX-treated H69AR cancer cells due

to the overexpression of ABC transporters on the surface of MDR cells.[60] Notably, the fluorescence in the NC NEPMs- and DOX-PLLA PMs-treated H69AR cancer cells is similar to that of the cells treated with free DOX.[61] In particular, the ultimate target site of DOX is nuclei, where it forms a DNA-DOX adduct to inhibit its transcription and subsequently proliferation and induce the death of cells. We demonstrate that the accumulation of DOX in the nuclei would certainly improve the antiproliferative effect of the cancer cell.

The promotion of the siRNA release from the siRNA-CS nanoparticles into cell cytosol is critical for effective RNA interference. With the purpose of better understanding that whether the siRNA could release from nanoparticles and escape from the lysosome successfully. Lysosomes and siRNA were labeled by LysoTracker Red and FAM, respectively. As shown in Figure 6, siRNA-CS nanoparticles were taken up efficiently as signified by the strong green signal. More importantly, FAM-siRNA was separated from the red spots (LysoTracker Red), confirming the successful escape from the lysosomes. The escape from the lysosome could be due to the ability of CS nanoparticles that mediates the endosomal escape through the proton sponge effect.[62] These results demonstrate that the siRNA-CS nanoparticles not only showed high uptake by H69AR cells but also promoted siRNA release in the cytosol through lysosomal escape.

Anticancer efficacy

Preceding studies indicated that siRNAs had improved the antitumor effects along with the conventional chemotherapeutic agents.[63] To quantitatively elucidate the antiproliferative efficacy of NEPMs, we investigated the viability of H69AR cancer cells using the MTT assay along with the free DOX, NC NEPMs, and DOX-PLLA PMs. As shown in Figure 7, the viable count of cells is >80% even at the concentration of 10 μg/mL after 24 hours of incubation with the free DOX due to the overexpression of MDR efflux pumps on the surface and the internalized DOX molecules being retreated by them.[60] Contrariwise, the NEPMs loaded with MRP1 siRNA and DOX were significantly more efficient in inhibiting the cell growth of MDR cells compared with that of the NC NEPMs and DOX-PLLA PMs treatment. The NEPMs treatment in MDR cells has shown the cell viability of ~46% at an equivalent DOX concentration of 7.5 μg/mL, while the corresponding cell viabilities of free DOX, DOX-PLLA PMs, and NC NEPMs remained 80.46%, 95.98%, and 96.94%, respectively. The results demonstrate that the codelivery of DOX and siRNA could obviously improve their therapeutic efficacy compared with that of DOX alone in the MDR cells due to the gene silencing effect of MRP1 siRNA in the cells

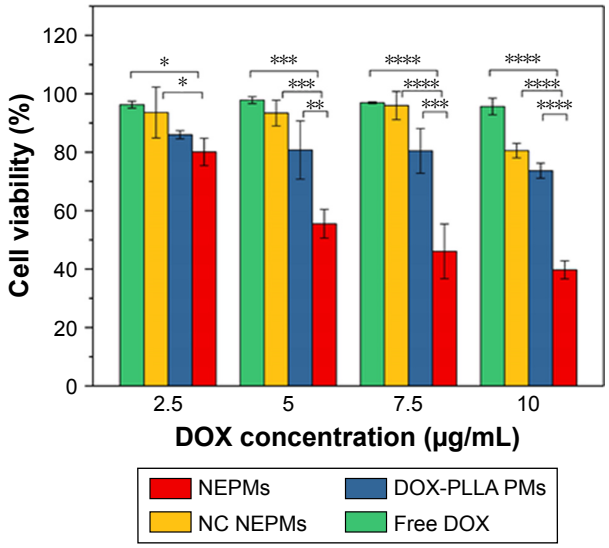

Figure 7 Evaluation of the antiproliferative effect of NEPMs.
Notes: Graphical representation illustrating the cell viability count of H69AR cancer cells after treatment with various sample combinations of NEPMs at an equivalent concentration of DOX. *Statistical significance, $P<0.05$; **$P<0.01$; ***$P<0.001$; ****$P<0.0001$.
Abbreviations: DOX, doxorubicin hydrochloride; NC, negative control; NEPM, nano-embedded porous microparticle; PM, porous microparticle; PLLA, poly-L-lactide.

and then increase their sensitivity to DOX.[64] PLLA and CS are generally considered as biocompatible substrates, which are predominantly utilized for the fabrication of drug delivery systems. However, the parameters or processing effects may sometimes result in the compatibility issues. To evaluate the biocompatibility of SCF-processed PMs, we performed the cytotoxicity assay of naked NEPMs on fibroblast cells (L929 cells). The CS-PLLA PMs at different concentrations had shown no significant influence on the viability of cells at different incubation times, which was consistent with the known biocompatibility of PLLA and CS (Figure S1). Moreover, these results can be correlated with the eco-friendly nature of SCF processing, demonstrating that the PMs based on the SAS process with no organic solvent residue in the eventual composites have no chance for causing lung damage after pulmonary administration, promoting potential application in pulmonary drug delivery.[34,39]

Conclusion

In summary, we successfully developed an inhalation codelivery system based on NEPMs through an eco-friendly SAS process for simultaneous delivery of an anticancer drug and siRNA to overcome MDR in lung tumor. These NEPMs with excellent biocompatibility and aerodynamic properties have delivered both the agents in a controlled release fashion and are optimum for the pulmonary delivery. Compared with free DOX, NEPMs have enhanced the antiproliferative effects efficiently on DOX by conquering the

MDR in the lung cancer cells. This eco-friendly approach provides a convenient way for the fabrication of inhalation codelivery system based on PMs with the combination of chemotherapy and gene therapy technology in the treatment of lung cancer.

Acknowledgments

Financial support from the National Natural Science Foundation of China (31470927, U1605225 and 31570974), Public Science and Technology Research Funds Projects of Ocean (201505029), Promotion Program for Young and Middle-aged Teacher in Science and Technology Research of Huaqiao University (ZQN-PY107), and Subsidized Project for Cultivating Postgraduates' Innovative Ability in Scientific Research of Huaqiao University is gratefully acknowledged.

Disclosure

The authors report no conflicts of interest in this work.

References

1. Spiro SG, Tanner NT, Silvestri GA, et al. Lung cancer: progress in diagnosis, staging and therapy. *Respirology*. 2010;15(1):44–50.
2. Berger W, Setinek U, Hollaus P, et al. Multidrug resistance markers P-glycoprotein, multidrug resistance protein 1, and lung resistance protein in non-small cell lung cancer: prognostic implications. *J Cancer Res Clin Oncol*. 2005;131(6):355–363.
3. Siegel RL, Miller KD, Jemal A. Cancer statistics, 2017. *CA Cancer J Clin*. 2017;67(1):7–30.
4. Wagner TD, Yang GY. The role of chemotherapy and radiation in the treatment of locally advanced non-small cell lung cancer (NSCLC). *Curr Drug Targets*. 2010;11(1):67–73.
5. Katzel JA, Fanucchi MP, Li Z, Zj L. Recent advances of novel targeted therapy in non-small cell lung cancer. *J Hematol Oncol*. 2009;2(1):2.
6. Kankala RK, Tsai P-Y, Kuthati Y, Wei P-R, Liu C-L, Lee C-H. Overcoming multidrug resistance through co-delivery of ROS-generating nano-machinery in cancer therapeutics. *J Mater Chem B*. 2017;5(7):1507–1517.
7. Wu H, Hait WN, Yang JM. Small interfering RNA-induced suppression of MDR1 (P-glycoprotein) restores sensitivity to multidrug-resistant cancer cells. *Cancer Res*. 2003;63(7):1515–1519.
8. Chen ZS, Tiwari AK. Multidrug resistance proteins (MRPs/ABCCs) in cancer chemotherapy and genetic diseases. *Febs J*. 2011;278(18):3226–3245.
9. Kankala RK, Liu C-G, Chen A-Z, et al. Overcoming multidrug resistance through the synergistic effects of hierarchical pH-sensitive, ROS-generating nanoreactors. *ACS Biomater Sci Eng*. 2017;3(10):2431–2442.
10. Gao Y, Chen Y, Ji X, Xf J, et al. Controlled intracellular release of doxorubicin in multidrug-resistant cancer cells by tuning the shell-pore sizes of mesoporous silica nanoparticles. *ACS Nano*. 2011;5(12):9788–9798.
11. Li W, Zhang H, Assaraf YG, et al. Overcoming ABC transporter-mediated multidrug resistance: molecular mechanisms and novel therapeutic drug strategies. *Drug Resist Updat*. 2016;27:14–29.
12. Wang D, Xu X, Zhang K, et al. Codelivery of doxorubicin and MDR1-siRNA by mesoporous silica nanoparticles-polymerpolyethylenimine to improve oral squamous carcinoma treatment. *Int J Nanomedicine*. 2018;13:187–198.
13. Saad M, Garbuzenko OB, Minko T. Co-delivery of siRNA and an anticancer drug for treatment of multidrug-resistant cancer. *Nanomedicine*. 2008;3(6):761–776.
14. Taratula O, Garbuzenko O, Savla R, Wang YA, He H, Minko T. Multifunctional nanomedicine platform for cancer specific delivery of siRNA by superparamagnetic iron oxide nanoparticles-dendrimer complexes. *Curr Drug Deliv*. 2011;8(1):59–69.
15. Li J, Liu J, Guo N, Zhang X. Reversal of multidrug resistance in breast cancer MCF-7/ADR cells by h-R3-siMDR1-PAMAM complexes. *Int J Pharm*. 2016;511(1):436–445.
16. Kesharwani P, Gajbhiye V, Jain NK. A review of nanocarriers for the delivery of small interfering RNA. *Biomaterials*. 2012;33(29):7138–7150.
17. Mishra DK, Balekar N, Mishra PK. Nanoengineered strategies for siRNA delivery: from target assessment to cancer therapeutic efficacy. *Drug Deliv Transl Res*. 2017;7(2):346–358.
18. Meng H, Mai WX, Zhang H, et al. Codelivery of an optimal drug/siRNA combination using mesoporous silica nanoparticles to overcome drug resistance in breast cancer in vitro and in vivo. *ACS Nano*. 2013;7(2):994–1005.
19. Liu J, Li J, Liu N, et al. In vitro studies of phospholipid-modified PAMAM-siMDR1 complexes for the reversal of multidrug resistance in human breast cancer cells. *Int J Pharm*. 2017;530(1–2):291–299.
20. Azarmi S, Roa WH, Löbenberg R. Targeted delivery of nanoparticles for the treatment of lung diseases. *Adv Drug Deliv Rev*. 2008;60(8):863–875.
21. Pooja D, Kulhari H, Kuncha M, et al. Improving efficacy, oral bioavailability, and delivery of paclitaxel using protein-grafted solid lipid nanoparticles. *Mol Pharm*. 2016;13(11):3903–3912.
22. Zhou QT, Tang P, Leung SS, Chan JG, Chan HK. Emerging inhalation aerosol devices and strategies: where are we headed? *Adv Drug Deliv Rev*. 2014;75:3–17.
23. Taratula O, Kuzmov A, Shah M, Garbuzenko OB, Minko T. Nanostructured lipid carriers as multifunctional nanomedicine platform for pulmonary co-delivery of anticancer drugs and siRNA. *J Control Release*. 2013;171(3):349–357.
24. Lam JK, Liang W, Chan HK. Pulmonary delivery of therapeutic siRNA. *Adv Drug Deliv Rev*. 2012;64(1):1–15.
25. Rogliani P, Calzetta L, Coppola A, et al. Optimizing drug delivery in COPD: the role of inhaler devices. *Respir Med*. 2017;124:6–14.
26. Al-Hallak MH, Sarfraz MK, Azarmi S, Roa WH, Finlay WH, Löbenberg R. Pulmonary delivery of inhalable nanoparticles: dry powder inhalers. *Ther Deliv*. 2011;2(10):1313–1324.
27. Tan SJ, Kiatwuthinon P, Roh YH, Kahn JS, Luo D. Engineering nanocarriers for siRNA delivery. *Small*. 2011;7(7):841–856.
28. Abdelaziz HM, Gaber M, Abd-Elwakil MM, et al. Inhalable particulate drug delivery systems for lung cancer therapy: nanoparticles, microparticles, nanocomposites and nanoaggregates. *J Control Release*. 2018;269:374–392.
29. Nascimento TL, Hillaireau H, Fattal E. Nanoscale particles for lung delivery of siRNA. *J Drug Deliv Sci Technol*. 2012;22(1):99–108.
30. Loira-Pastoriza C, Todoroff J, Vanbever R. Delivery strategies for sustained drug release in the lungs. *Adv Drug Deliv Rev*. 2014;75:81–91.
31. Fiore VF, Lofton MC, Roser-Page S, et al. Polyketal microparticles for therapeutic delivery to the lung. *Biomaterials*. 2010;31(5):810–817.
32. Vanbever R, Mintzes JD, Wang J, et al. Formulation and physical characterization of large porous particles for inhalation. *Pharm Res*. 1999;16(11):1735–1742.
33. Menon JU, Ravikumar P, Pise A, Gyawali D, Hsia CC, Nguyen KT. Polymeric nanoparticles for pulmonary protein and DNA delivery. *Acta Biomater*. 2014;10(6):2643–2652.
34. Wang Y, Zhu L-H, Chen A-Z, Xu Q, Hong Y-J, Wang S-B. One-step method to prepare PLLA porous microspheres in a high-voltage electrostatic anti-solvent process. *Materials*. 2016;9(5):368.
35. D'Angelo I, Casciaro B, Miro A, Quaglia F, Mangoni ML, Ungaro F. Overcoming barriers in Pseudomonas aeruginosa lung infections: engineered nanoparticles for local delivery of a cationic antimicrobial peptide. *Colloids Surf B Biointerfaces*. 2015;135:717–725.

36. Kaye RS, Purewal TS, Alpar HO. Simultaneously manufactured nano-in-micro (SIMANIM) particles for dry-powder modified-release delivery of antibodies. *J Pharm Sci*. 2009;98(11):4055–4068.
37. Price DN, Stromberg LR, Kunda NK, Muttil P. In vivo pulmonary delivery and magnetic-targeting of dry powder nano-in-microparticles. *Mol Pharm*. 2017;14(12):4741–4750.
38. Lee HJ, Kang JH, Lee HG, et al. Preparation and physicochemical characterization of spray-dried and jet-milled microparticles containing bosentan hydrate for dry powder inhalation aerosols. *Drug Des Devel Ther*. 2016;10:4017–4030.
39. Chen A-Z, Tang N, Wang S-B, Kang Y-Q, Song H-F. Insulin-loaded poly-L-lactide porous microspheres prepared in supercritical CO_2 for pulmonary drug delivery. *J Supercrit Fluids*. 2015;101:117–123.
40. Kankala RK, Zhang YS, Wang SB, Lee CH, Chen AZ. Supercritical fluid technology: an emphasis on drug delivery and related biomedical applications. *Adv Healthc Mater*. 2017;6(16):31.
41. Chen BQ, Kankala RK, Chen AZ, et al. Investigation of silk fibroin nanoparticle-decorated poly(L-lactic acid) composite scaffolds for osteoblast growth and differentiation. *Int J Nanomedicine*. 2017;12:1877–1890.
42. Mizuno T, Mohri K, Nasu S, Danjo K, Okamoto H. Dual imaging of pulmonary delivery and gene expression of dry powder inhalant by fluorescence and bioluminescence. *J Control Release*. 2009;134(2):149–154.
43. Esfandiari N. Production of micro and nano particles of pharmaceutical by supercritical carbon dioxide. *J Supercrit Fluids*. 2015;100:129–141.
44. Restani RB, Silva AS, Pires RF, et al. Nano-in-micro poxylated polyurea dendrimers and chitosan dry powder formulations for pulmonary delivery. *Part Part Syst Charact*. 2016;33(11):851–858.
45. Silva AS, Tavares MT, Aguiar-Ricardo A. Sustainable strategies for nano-in-micro particle engineering for pulmonary delivery. *J Nanopart Res*. 2014;16(11):17.
46. Ali ME, Lamprecht A. Spray freeze drying for dry powder inhalation of nanoparticles. *Eur J Pharm Biopharm*. 2014;87(3):510–517.
47. Chen A-Z, Kang Y-Q, Wang S-B, Tang N, Su X-Q, Xq S. Preparation and antitumor effect evaluation of composite microparticles co-loaded with siRNA and paclitaxel by a supercritical process. *J Mater Chem B*. 2015;3(31):6439–6447.
48. Chen A-Z, Zhao C, Wang S-B, Liu Y-G, Lin D-L. Generation of porous poly-L-lactide microspheres by emulsion-combined precipitation with a compressed CO_2 antisolvent process. *J Mater Chem B*. 2013;1(23):2967–2975.
49. Kang YQ, Zhao C, Chen AZ, et al. Study of lysozyme-loaded poly-L-lactide (PLLA) porous microparticles in a compressed CO_2 antisolvent process. *Materials*. 2013;6(8):3571–3583.
50. Taki M, Marriott C, Zeng XM, Martin GP. Aerodynamic deposition of combination dry powder inhaler formulations in vitro: a comparison of three impactors. *Int J Pharm*. 2010;388(1–2):40–51.
51. Cuong N-V, Li Y-L, Hsieh M-F. Targeted delivery of doxorubicin to human breast cancers by folate-decorated star-shaped PEG–PCL micelle. *J Mater Chem*. 2012;22(3):1006–1020.
52. Hashad RA, Ishak RA, Fahmy S, Mansour S, Geneidi AS. Chitosan-tripolyphosphate nanoparticles: optimization of formulation parameters for improving process yield at a novel pH using artificial neural networks. *Int J Biol Macromol*. 2016;86:50–58.
53. Csaba N, Köping-Höggård M, Alonso MJ. Ionically crosslinked chitosan/tripolyphosphate nanoparticles for oligonucleotide and plasmid DNA delivery. *Int J Pharm*. 2009;382(1–2):205–214.
54. Das G, Nicastri A, Coluccio ML, et al. FT-IR, Raman, RRS measurements and DFT calculation for doxorubicin. *Microsc Res Tech*. 2010;73(10):991–995.
55. Scj L, Ooi CP, Boey YCF. Radiation effects on poly(lactide-co-glycolide) (PLGA) and poly(L-lactide) (PLLA). *Polym Degradation Stab*. 2004;83(2):259–265.
56. Kim I, Byeon HJ, Kim TH, et al. Doxorubicin-loaded highly porous large PLGA microparticles as a sustained-release inhalation system for the treatment of metastatic lung cancer. *Biomaterials*. 2012;33(22):5574–5583.
57. Kim H, Lee J, Kim TH, et al. Albumin-coated porous hollow poly(lactic-co-glycolic acid) microparticles bound with palmityl-acylated exendin-4 as a long-acting inhalation delivery system for the treatment of diabetes. *Pharm Res*. 2011;28(8):2008–2019.
58. Kang Y, Yang C, Ouyang P, Ping OY, et al. The preparation of BSA-PLLA microparticles in a batch supercritical anti-solvent process. *Carbohydr Polym*. 2009;77(2):244–249.
59. Alibolandi M, Abnous K, Hadizadeh F, et al. Dextran-poly lactide-co-glycolide polymersomes decorated with folate-antennae for targeted delivery of docetaxel to breast adenocarcinima in vitro and in vivo. *J Control Release*. 2016;241:45–56.
60. Guo L, Liu Y, Bai Y, Sun Y, Xiao F, Guo Y. Gene expression profiling of drug-resistant small cell lung cancer cells by combining microRNA and cDNA expression analysis. *Eur J Cancer*. 2010;46(9):1692–1702.
61. Lin S, Deng F, Huang P, et al. A novel legumain protease-activated micelle cargo enhances anticancer activity and cellular internalization of doxorubicin. *J Mater Chem B*. 2015;3(29):6001–6012.
62. Richard I, Thibault M, de Crescenzo G, Buschmann MD, Lavertu M. Ionization behavior of chitosan and chitosan-DNA polyplexes indicate that chitosan has a similar capability to induce a proton-sponge effect as PEI. *Biomacromolecules*. 2013;14(6):1732–1740.
63. Deng X, Cao M, Zhang J, et al. Hyaluronic acid-chitosan nanoparticles for co-delivery of MiR-34a and doxorubicin in therapy against triple negative breast cancer. *Biomaterials*. 2014;35(14):4333–4344.
64. Fan YP, Liao JZ, Lu YQ, Yq L, et al. MiR-375 and doxorubicin co-delivered by liposomes for combination therapy of hepatocellular carcinoma. *Mol Ther Nucleic Acids*. 2017;7:181–189.

Supplementary material

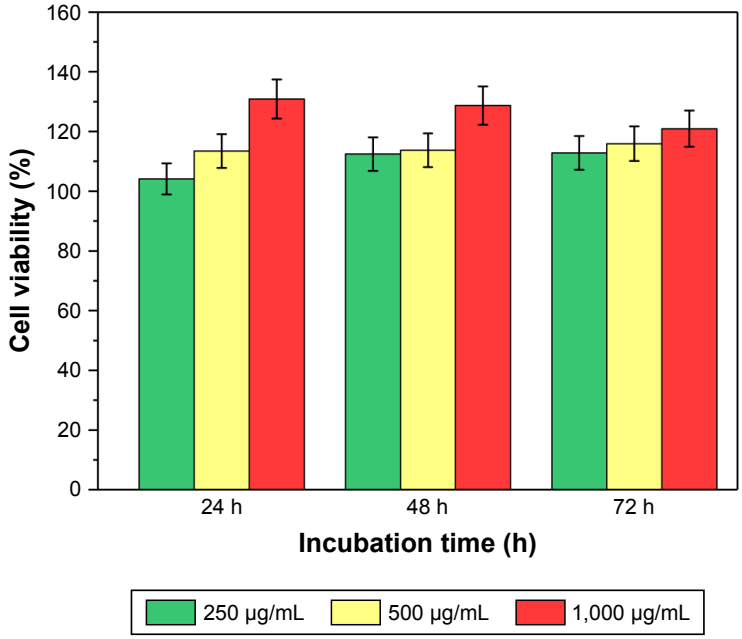

Figure S1 Relative cell viability of L929 cells after treatment with naked NEPMs.
Notes: Cells were seeded at a density of 5×10^4 cells per well of a 96-well plate and incubated overnight for proper attachment. The cultured media was then replaced with the media containing CS-PLLA PMs at different concentrations (250, 500, and 1,000 µg/mL) exposed for different time intervals (24, 48, and 72 hours). The viability of cells was then measured following the MTT assay procedure (see Anticancer study).